

# On global properties of time–delayed feedback control: weakly nonlinear analysis

Wolfram Just<sup>1</sup>

*Queen Mary / University of London, School of Mathematical Sciences, Mile End Road, London E1 4NS, UK*

Hartmut Benner and Clemens von Loewenich

*Institute for Solid State Physics, Darmstadt University of Technology, Hochschulstraße 6, D-64289 Darmstadt, Germany*

---

## Abstract

We address the problem which type of initial state yields successful stabilisation when time–delayed feedback control is applied. Using well known concepts from bifurcation theory we provide a general mechanism that limits the corresponding basins of attraction. Application of normal form analysis to general delay–differential equations proves the universality of our results. The empirical criteria which determine the prospective size of the basin are easily accessible and a demonstration in terms of a simple numerical simulation is provided.

*Key words:* control of chaos, differential–difference equations, codimension two bifurcations, hysteresis

---

## 1 Introduction

The field of Control of Chaos, as it has been introduced by the pioneering work of the Maryland group [1], has developed during the last decade into one of the most active fields in applied nonlinear science. Although control theory is a well developed discipline in applied mathematics and engineering science [2–4] some new aspects have been emphasised in the physics literature, like noninvasive control for stabilising the vast number of unstable periodic orbits embedded in a chaotic attractor or the use of invariant manifolds for

---

<sup>1</sup> e–mail: W.Just@qmul.ac.uk

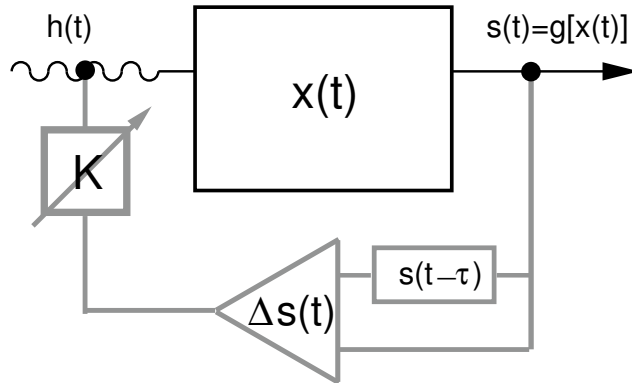


Fig. 1. Setup of time–delayed feedback control.  $h(t)$ : system parameter,  $x(t)$ : internal degrees of freedom,  $s(t) = g[x(t)]$ : measured signal. The time delay feedback loop is displayed in grey.

optimising control performance (cf. e.g. [5]). Last but not least an extremely simple control scheme has been proposed [6] which allows the stabilisation of time–periodic states when no a priori information about the internal dynamics of the system is available. It is just based on the online measurement of a single signal and requires a time–delayed difference for constructing an appropriate control force. Although the method is in principle inferior to standard approaches in control theory its strength comes from the fact that no fancy data processing is required and that the method is very robust. It has been applied successfully in experiments as diverse as hydrodynamics [7], lasers [8], ferromagnetic resonance [9], or electrochemical setups [10]. In each case the control scheme consists in measuring a single signal  $s(t)$ , taking the time delayed difference  $s(t) - s(t - \tau)$ , and using this control signal to modulate one parameter of the system. In order to have a simple control parameter one usually just amplifies the control signal by some factor  $K$  and adjusts the control amplitude  $K$  such that successful stabilisation of a time periodic state occurs. When the delay time is chosen as an (integer) multiple of the period of the target state the control scheme is clearly noninvasive since the control force  $K[s(t) - s(t - \tau)]$  vanishes when the target state is reached. A diagrammatic view of the control setup is shown in figure 1.

Although the experimental implementation of time–delayed feedback control is almost trivial, the price one has to pay from the theoretical point of view is that the discussion of time–delayed feedback schemes requires the analysis of differential–difference equations. Such systems are quite difficult to handle since the dynamics takes place in infinite–dimensional phase spaces [11]. The standard tool for discussing the control performance consists in linear stability analysis. Even such a straightforward approach has been worked out for time–delayed feedback schemes only recently [12–14]. As a particular benefit of such concepts one has now gained a quite complete overview of the control performance of time–delayed feedback control from the local point of view (cf. e.g. [15] for recent reviews).

What is however still missing are general results concerning global properties of time–delayed feedback systems. For instance, it is completely unclear how large basins of attraction are, i.e. which initial condition is attracted towards a particular stabilised orbit. For time local control schemes such topics are addressed by control theory and substantial results are available in the literature, although one has to keep in mind that basins of attraction may have an incredibly complicated topology [16]. But for time–delay systems phase spaces are infinite dimensional and even the visualisation of trajectories becomes a challenge [17]. In applications and simulations one usually resorts to the fact that chaotic dynamics is ergodic and a trajectory visits a neighbourhood of each periodic orbit with finite probability. Turning on the control loop only when such a neighbourhood is visited, i.e. when the control signal falls beyond a certain threshold one may obtain stabilisation. Apart from the fact that such an idea is far from being a systematic treatment it can only be applied in experimental systems when the amount of noise is small. Thus a detailed study of basins of attraction for time–delayed feedback control is a desirable task.

Since the analysis of basins of attraction in dynamical systems is usually a complicated task one cannot expect that we give an ultimate answer here. Our approach is just a first step and we intend to point out a generic mechanism which will determine basins of attraction in time–delayed feedback schemes. The key idea we are following comes from bifurcation theory. Thus one can expect that our results share some degree of universality and do not depend on the details of the underlying dynamics.

On changing the control amplitude  $K$  the former unstable periodic state may become stable and a control interval is obtained. At the boundaries of such a region bifurcations occur. In the generic case either a flip (i.e. period doubling) or a Hopf instability [18] appears provided the orbit obeys certain technical constraints. Among these instabilities there are two different types possible: either a continuous or a discontinuous transition, i.e. a super– or a subcritical bifurcation. Depending on that type a mechanism comes into play which creates a boundary for the basin of attraction (cf. figure 2). To illustrate the main idea in simple terms we resort for the moment to the stabilisation of fixed points instead of time periodic orbits. However, the bifurcation theoretical argument we are going to supply applies in the latter case as well<sup>2</sup>. Assume that at the upper control threshold  $K_{ho}$  a Hopf bifurcation appears, i.e. stabilisation occurs for  $K < K_{ho}$ . If the bifurcation is supercritical then at  $K_{ho}$  a stable limit cycle is born which extends to the region  $K > K_{ho}$ . In physical terms it means that the Fourier spectrum of the control system displays sidebands and a modulation instability occurs (cf. [19] for some experimental

---

<sup>2</sup> If one considers Hopf bifurcations of periodic orbits, then instead of a limit cycle a torus solution is created by the bifurcation.

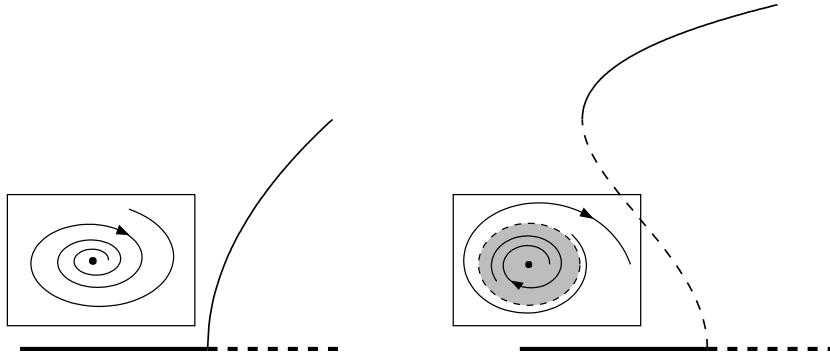


Fig. 2. Diagrammatic view of bifurcation diagrams for a supercritical (left) and a subcritical (right) Hopf instability. Stable/unstable fixed point: thick solid/dashed line, stable/unstable limit cycle: thin solid/dashed line. Inserts show phase space plots slightly below the threshold. The basin of attraction bounded by the unstable limit cycle is shaded.

results). If however the Hopf bifurcation is subcritical then the linearly stable state collides at  $K_{ho}$  with an unstable limit cycle which was already present in the control region  $K < K_{ho}$ . Beyond  $K_{ho}$  the dynamics jumps discontinuously to some coexisting attractor. Thus one obtains hysteresis when sweeping the control amplitude through the transition point  $K_{ho}$ . The unstable limit cycle (or more precisely: the stable manifold of this limit cycle) which is already present in the stable domain yields the basin boundary of the stabilised state. More seriously, since the limit cycle contracts to the stabilised state when the control threshold  $K_{ho}$  is reached the basin becomes small when  $K_{ho}$  is approached. Thus depending on the type of transition basins of attraction of different size appear. As these arguments are based on bifurcation theory they are universal and even apply to time-delay systems [11]. Of course we have to confess that this argument still relies on local properties since we are dealing with the neighbourhood of the instability. But the global properties may be obtained in principle by continuation<sup>3</sup>. Thus we expect that parts of the analysis survive in larger distance from instability.

To summarise the essential idea, we expect that the basin of attraction is large, i.e. most initial conditions lead to stabilisation, when a continuous transition at the control boundary appears. On the other hand a discontinuous transition at the control boundary indicates that stabilisation works only in some neighbourhood of the target state. Such conditions can be easily checked by numerical simulations, whereas a proper theoretical approach calls for analysing the instability in terms of weakly nonlinear analysis, a standard technique in bifurcation theory. Our presentation will exactly follow such a reasoning.

<sup>3</sup> The actual numerical computation of the corresponding high dimensional stable manifold is extremely tedious. It is still beyond the capability of standard software tools.

## 2 Illustration by numerical simulations

The simplest dynamical toy models to which time–delayed feedback control can be applied are time discrete maps. They are easier to handle since the dimension of phase space stays to be finite even if the control loop is included. Thus visualisation of global properties remains feasible in such cases. For the purpose of illustration we consider the Henon map

$$\begin{aligned}x_{n+1} &= 1 - ax_n^2 + by_n + h(KF_n) \\ y_{n+1} &= x_n\end{aligned}\tag{1}$$

at parameter values  $a = 1.5$ ,  $b = 0.2$ . A control force  $F_n$  is applied for stabilisation of the fixed point  $x_* = y_*$  where  $2ax_* = -1 + b + \sqrt{4a + (1 - b)^2}$ . In order to avoid artifacts induced by unbounded trajectories we have introduced a cutoff of the control force at an amplitude  $\rho = 0.4$  through the coupling function  $h(z) = z$  if  $|z| < \rho$  and  $h(z) = \rho \text{sign}(z)$  if  $|z| \geq \rho$ . The simplest time–delayed feedback scheme for stabilising the fixed point corresponds to the choice  $F_n = x_n - x_{n-1}$ . For our purpose it is however more appropriate to resort to control schemes with two parameters. A very prominent example of such a scheme involves multiple delay terms  $x_{n-k} - x_{n-k-1}$  weighted by an exponentially decaying factor  $R^k$ . Such extended control schemes have been introduced for the purpose of stabilising fast chaotic systems [20], and these concepts are quite well established in standard control theory. For the present example the scheme may be written as

$$F_{n+1} = x_{n+1} - x_n + RF_n \quad .\tag{2}$$

For the choice  $R = 0$  the original time–delayed feedback scheme proposed by Pyragas is recovered. Eqs.(1) and (2) constitute a three dimensional map which is quite simple to handle and even global features are accessible.

The linear stability analysis for the fixed point is a trivial task. Straightforward calculation tells us that stability occurs in a finite interval  $[K_{\text{fl}}, K_{\text{ho}}]$  of control amplitudes where the lower threshold is given by

$$K_{\text{fl}} = -\frac{1}{2}(1 - b - 2ax_*)(1 + R)\tag{3}$$

and the upper threshold reads

$$K_{\text{ho}} = \frac{1 + 2ax_*R - bR(R + bR - 2ax_*) + b}{1 + bR} \quad .\tag{4}$$

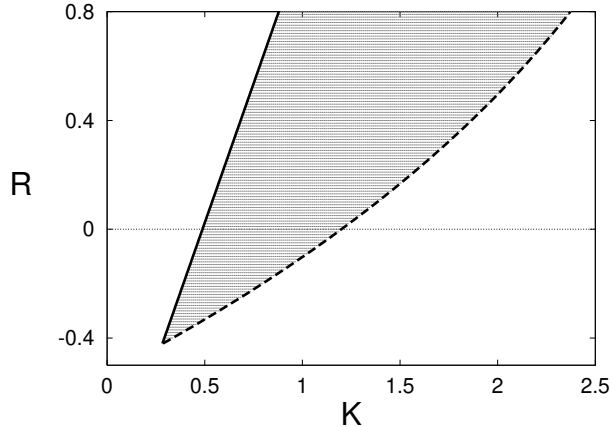


Fig. 3. Region of linear stability of the Henon map (1) for extended control (2) of the fixed point. Full line: lower threshold, eq.(3), dashed line: upper threshold, eq.(4). Dots indicate results of successful stabilisation in simulations with initial condition in the immediate vicinity of the fixed point.

The lower threshold (3) yields a flip bifurcation since the corresponding instability is governed by a single negative eigenvalue whereas the upper threshold (4) yields a Hopf instability caused by a complex conjugated pair. The domain of stability in the control parameter plane is shown in figure 3.

The geometry of the control domain shows the generic triangular shape which can be reproduced for quite general systems by analytical approaches<sup>4</sup>. The lower threshold yields a straight line in the  $K$ - $R$  diagram which is in fact a rigorous result for any system [18]. The precise shape of the upper control threshold depends on the particular dynamics and its precise form may strongly vary for different models [12,21]. Let us now have a closer look on the control boundaries, when sweeping the control amplitude  $K$  across the critical values  $K_{fl}$  or  $K_{ho}$ . Approaching the lower threshold from below we observe an inverse period doubling cascade which finally terminates in the stabilised periodic orbit (cf. figure 4). The transition is continuous, i.e. supercritical, and such a feature is observed regardless of the particular value of the filter parameter  $R$ . Thus no transition from supercritical to subcritical behaviour takes place on the left hand boundary of the control domain. In fact, as will be shown in the next section such a property is a generic feature of time-delayed feedback control which is independent on the particular system under study.

The situation is completely different at the upper control threshold (cf. figure 5). Comparing the behaviour for different values of  $R$  one obtains a continuous transition, i.e. a supercritical Hopf instability, at negative  $R$  whereas for positive  $R$  the transition becomes discontinuous. For  $R = 0.2$  the systems jumps to a period 4 state and even a tiny region of bistability is visible. Thus there

<sup>4</sup> To be precise: such a geometry appears if unstable periodic orbits with a negative Floquet multiplier are considered so that the unstable manifold is a Möbius strip.

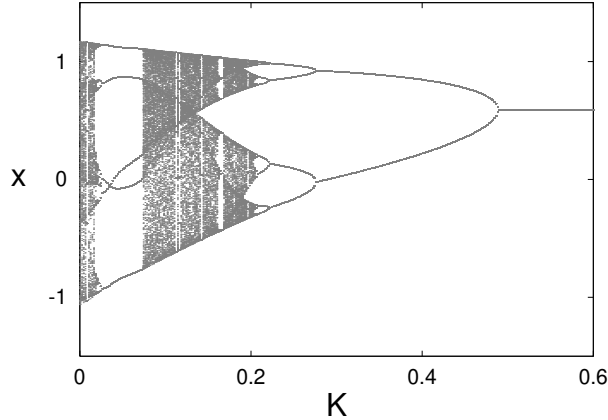


Fig. 4. Bifurcation diagram for the Henon map in dependence on the control amplitude  $K$  in a neighbourhood of the lower control threshold  $K_{\text{fl}}$  for  $R = 0$ .

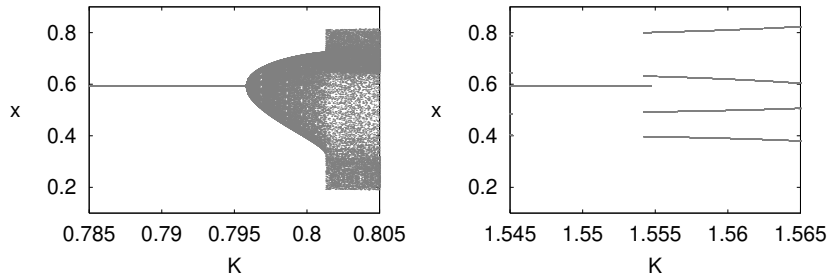


Fig. 5. Bifurcation diagrams for the Henon map in dependence on the control amplitude  $K$  in a neighbourhood of the upper control threshold  $K_{\text{ho}}$ . Left:  $R = -0.2$ , right:  $R = 0.2$ .

appears a transition from super- to subcritical behaviour. In fact using the approaches shown in the next section one may prove by analytical methods that the transition appears exactly at  $R = 0$ .

According to the general idea presented above we now expect that the basins of attraction differ in both cases considerably. As the full phase space is three-dimensional we have to compute three-dimensional sets. In order to reduce the effort we concentrate on a two-dimensional slice choosing  $F \equiv 0$ , i.e. we consider initial conditions with initial force  $F_0 = 0$ . Each point in the  $x_0$ - $y_0$  plane is recorded for which successful stabilisation occurs. Numerical results are displayed in figure 6 for two different  $R$ -values. In order to have a meaningful comparison between both cases we chose the control amplitude  $K$  in roughly the same distance from the corresponding control threshold  $K_{\text{ho}}$ . In the supercritical case,  $R = -0.2$  we observe a large basin of attraction. In fact all tested initial conditions yield stabilisation. For the subcritical case  $R = 0.2$  the situation differs substantially. The domain of attraction shows a fairly complicated structure and a substantial portion of initial conditions does not lock onto the target state. To confirm that such a domain is really related

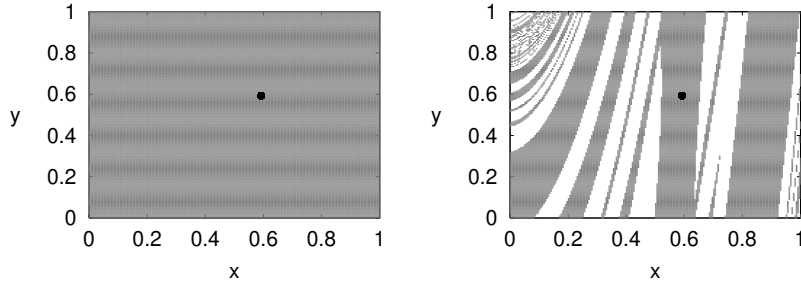


Fig. 6. Basin of attraction for the Henon map with initial force  $F_0 = 0$ . The fixed point is indicated by a full circle. Left:  $R = -0.2$ ,  $K = 0.79$ , right:  $R = 0.2$ ,  $K = 1.55$  (cf. figure 5).

to the subcritical instability one may study in detail how the morphology of the basin of attraction changes when  $K_{ho}$  is approached. In fact the domain finally becomes circular as predicted by the bifurcation theoretical argument. But such a detailed study is for our purpose not rewarding and it is beyond the scope of the present discussion.

Thus the numerical findings in this trivial model confirm the general idea presented above. However, it remains to be clarified when the sub–supercritical transition appears and which features of our numerical simulation are generic. Such a problem can be tackled by normal forms in terms of a weakly nonlinear perturbation expansion.

### 3 Normal form analysis

To analyse which features of the previous example are generic properties for time–delayed feedback control we have to resort to the general setup sketched in figure 1. If we denote the internal dynamical degrees of freedom by a state vector  $\mathbf{x}(t)$  then the equations of motion may be cast into the form

$$\dot{\mathbf{x}} = \mathbf{f}(\mathbf{x}(t), KF(t)) \quad (5)$$

where of course the functional form of the right hand side  $\mathbf{f}$  depends on the details of the system. The control force is generated from measured signal  $s(t) = g[\mathbf{x}(t)]$  by a time–delayed difference. It reads

$$F(t) = g[\mathbf{x}(t)] - g[\mathbf{x}(t - \tau)] + RF(t - \tau) \quad (6)$$

when the extended control scheme is applied. For the subsequent analysis it is more convenient to rewrite eq.(6) in its iterated form

$$F(t) = \sum_{k=0}^{\infty} R^k (g[\mathbf{x}(t - k\tau)] - g[\mathbf{x}(t - (k + 1)\tau)]) \quad (7)$$

which shows explicitly that the scheme is based on multiple delays. Without control force  $K = 0$  we presuppose that the system (5) possesses an unstable periodic orbit  $\boldsymbol{\xi}(t) = \boldsymbol{\xi}(t + \tau)$  which we intend to stabilise. Eqs.(5) and (7) constitute a differential–difference system. The linear stability analysis is quite straightforward [18]. Such an analysis confirms essentially the shape of the control domain found in the previous example, provided we restrict our discussion to an unstable orbit  $\boldsymbol{\xi}(t)$  having a single unstable negative Floquet multiplier.

In order to tackle the global features of the dynamics we need to analyse whether the bifurcations at the lower and the upper control threshold are sub– or supercritical. Such a question can be answered by normal form analysis where one reduces the full dynamics to an effective equation of motion

$$z'(\theta) = \mu z(\theta) - r|z(\theta)|^2 z(\theta) \quad (8)$$

on a slow time scale  $\theta$ . At the lower threshold, i.e. for the flip instability, the effective equation becomes one–dimensional and  $z(\theta)$  takes real values only, whereas at the upper threshold the complex number  $z(\theta)$  describes the dynamics on the two–dimensional centre manifold. Above all, the question whether these bifurcation are sub– or supercritical is solely determined by the sign of the real part of the cubic coefficient  $r$ . Positive values yield supercritical behaviour, negative values indicate a discontinuous transition. Thus the ultimate goal of the subsequent analysis is the computation of  $r$ . As our final result we will obtain that  $r$  is constant along the boundary which is determined by the flip instability, whereas the sign of  $\text{Re}(r)$  may change for the right–hand boundary caused by the Hopf bifurcation.

For computational purpose we need to write down the linear stability problem. Consider small deviations from the periodic orbit  $\delta\mathbf{x}(t) = \mathbf{x}(t) - \boldsymbol{\xi}(t)$ . Fixing the control amplitude to its critical value, i.e. either on a Hopf or on the flip bifurcation line  $K_c = K_{\text{fl/ho}}(R)$ , the deviations in linear order obey  $\delta\mathbf{x}(t) = \exp(i\Omega_c t)\mathbf{u}(t)$  where the eigenvalue problem

$$\begin{aligned} & \dot{\mathbf{u}}(t) + i\Omega_c \mathbf{u}(t) \\ &= \left[ D\mathbf{f}(\boldsymbol{\xi}(t), 0) + K_c \frac{1 - \exp(-i\Omega_c \tau)}{1 - R \exp(-i\Omega_c \tau)} d\mathbf{f}(\boldsymbol{\xi}(t), 0) \otimes Dg[\boldsymbol{\xi}(t)] \right] \mathbf{u}(t) \quad (9) \end{aligned}$$

determines the frequency  $\Omega_c$  and the time periodic amplitude  $\mathbf{u}(t) = \mathbf{u}(t + \tau)$ . Here the symbol  $D$  denotes derivatives with respect to the vector valued argument,  $d$  derivatives with respect to the scalar argument<sup>5</sup>, and  $\otimes$  indicates the outer product of two vector valued quantities. The eigenvalue problem (9) fixes the shape of the control domain. For the case of flip instabilities the critical frequency obeys  $\Omega_{\text{fl}} = \pi/\tau$ , i.e. its value is independent of  $R$ . As a consequence all quantities appearing in eq.(9) must be constant, in particular

$$\frac{2K_{\text{fl}}}{1+R} = \kappa = \text{const.}, \quad (\Omega_{\text{fl}} = \pi/\tau) \quad (10)$$

holds. Thus the corresponding boundary yields a straight line (cf. figure 3). As  $\Omega_c$  may change along the Hopf line no general statement can be made for the right-hand boundary.

If we go beyond the linear analysis higher order contributions have to be taken into account. Considering small deviations of the control amplitude from its critical value,  $K = K_c + \varepsilon^2 \delta K$ , we may perform an expansion in terms of the small parameter  $\varepsilon$  using a multiple scaling ansatz

$$\delta \mathbf{x}(t) = \frac{\varepsilon}{2} \left( z(\varepsilon^2 t) \exp(i\Omega_c t) \mathbf{u}(t) + \text{c.c.} \right) + \varepsilon^2 \delta \mathbf{x}_2(t) + \varepsilon^3 \delta \mathbf{x}_3(t) + \dots \quad (11)$$

Requiring that the higher order contributions  $\delta \mathbf{x}_k(t)$  remain bounded an equation of motion for the amplitude  $z$  on the slow time scale  $\theta = \varepsilon^2 t$  will be derived (cf. eq.(8)). Contrary to normal form calculations which are based on projection techniques, e.g. [22,23] for some recent applications, and which face severe technical problems when explicitly time dependent problems are addressed [11], the multiple scaling approach does not require the formulation of the equation of motion in a functional theoretic setting [24]. Inserting the ansatz (11) into eqs.(5) and (7) we recover in order  $\varepsilon$  the linear eigenvalue problem (9). To facilitate the subsequent calculation of the higher orders we first concentrate on the case of the flip instability. Comments concerning the Hopf bifurcation will be made at the end of this section.

It is special about the flip instability that the vector

$$\hat{\mathbf{u}}(t) = \exp(i\Omega_{\text{fl}} t) \mathbf{u}(t) \quad (12)$$

is a real valued quantity since  $\Omega_{\text{fl}} = \pi/\tau$  holds. This vector has a simple geometrical meaning since it points into the direction of the centre manifold (cf. eqs.(9) and (11)) which is given by a Möbius strip. Such a geometry is reflected by the condition of antiperiodicity,  $\hat{\mathbf{u}}(t) = -\hat{\mathbf{u}}(t + \tau)$  which follows in

<sup>5</sup> In components  $(D\mathbf{f}(\boldsymbol{\xi}, 0))_{\alpha\beta} = \partial f_{\alpha}(\boldsymbol{\xi}, 0)/\partial \xi_{\beta}$ ,  $(d\mathbf{f}(\boldsymbol{\xi}, 0))_{\alpha} = \partial f_{\alpha}(\boldsymbol{\xi}, F)/\partial F|_{F=0}$ .

a straightforward way from the value of the frequency and the periodicity of the eigenvector. Furthermore the amplitude  $z(\theta)$  becomes real valued as well. With these properties eq.(11) and the subsequent analysis simplifies.

Inserting eq.(11) into eqs.(5) and (7) we obtain in order  $\varepsilon^2$  an inhomogeneous linear equation for  $\delta\mathbf{x}_2(t)$

$$\begin{aligned} \delta\dot{\mathbf{x}}_2(t) &= D\mathbf{f}(\boldsymbol{\xi}(t), 0)\delta\mathbf{x}_2(t) \\ &+ d\mathbf{f}(\boldsymbol{\xi}(t), 0)K_{\text{fl}} \left( Dg[\boldsymbol{\xi}(t)] \sum_{k=0}^{\infty} [\delta\mathbf{x}_2(t - k\tau) - \delta\mathbf{x}_2(t - (k+1)\tau)] \right) \\ &+ \mathbf{I}_2(t)z^2(\theta) \end{aligned} \quad (13)$$

where the inhomogeneous part is given by<sup>6</sup>

$$\begin{aligned} \mathbf{I}_2(t) &= \frac{1}{2}D^2\mathbf{f}(\boldsymbol{\xi}(t), 0) : \hat{\mathbf{u}}(t) : \hat{\mathbf{u}}(t) : + Dd\mathbf{f}(\boldsymbol{\xi}(t), 0)\hat{\mathbf{u}}(t) \frac{2K_{\text{fl}}}{1+R}\sigma(t) \\ &+ \frac{1}{2}d^2\mathbf{f}(\boldsymbol{\xi}(t), 0) \left( \frac{2K_{\text{fl}}}{1+R} \right)^2 \sigma^2(t) \quad . \end{aligned} \quad (14)$$

Here the contributions coming from the derivative of the measured signal have been abbreviated by

$$\sigma(t) = Dg[\boldsymbol{\xi}(t)]\hat{\mathbf{u}}(t) \quad . \quad (15)$$

It is the essential point that the critical control amplitude  $K_{\text{fl}}$  and the filter parameter  $R$  just enter in the combination (10) which takes a constant value along the whole flip bifurcation line. Since  $\mathbf{I}_2(t)$  is periodic with period  $\tau$  no resonant contribution, i.e a term proportional to  $\exp(i\Omega_{\text{fl}}t)$ , appears<sup>7</sup>. Thus we may solve eq.(13) by

$$\delta\mathbf{x}_2(t) = \boldsymbol{\Gamma}(t)z^2(\theta), \quad \boldsymbol{\Gamma}(t) = \boldsymbol{\Gamma}(t + \tau) \quad (16)$$

where according to the multiple scaling technique the amplitude  $z(\theta)$  is treated as a constant on the time scale of order one. Plugging eq.(16) into eq.(13) we obtain observing the periodicity of  $\boldsymbol{\Gamma}(t)$

$$\dot{\boldsymbol{\Gamma}}(t) = D\mathbf{f}(\boldsymbol{\xi}(t), 0)\boldsymbol{\Gamma}(t) + d\mathbf{f}(\boldsymbol{\xi}(t), 0)\kappa(Dg[\boldsymbol{\xi}(t)]\boldsymbol{\Gamma}(t)) + \mathbf{I}_2(t) \quad . \quad (17)$$

<sup>6</sup> Second order derivatives are indicated by  $D^2$ ,  $Dd$ ,  $d^2$ , e.g. using components  $(D^2\mathbf{f}(\boldsymbol{\xi}, 0) : \mathbf{u} : \mathbf{v})_{\alpha} = \sum_{\beta\gamma} \partial^2 f_{\alpha}(\boldsymbol{\xi}, 0) / \partial(\xi_{\beta}\partial\xi_{\gamma}) u_{\beta}v_{\gamma}$ .

<sup>7</sup> We do not take the Goldstone mode into account which appears in autonomous models. Thus strictly speaking our analysis applies to periodically driven systems.

Although the expressions determining  $\mathbf{\Gamma}(t)$  look fairly complicated, cf. eqs.(14), (15), and (17), its value is solely determined by the parameter  $\kappa$  which is a constant along the flip bifurcation line.

Proceeding to the third order we have to observe that when inserting eq.(11) into eqs.(5) and (7) we get various contributions taking the second order result (16) into account. Finally we end up with an inhomogeneous equation for  $\delta\mathbf{x}_3(t)$  which reads

$$\begin{aligned} \delta\dot{\mathbf{x}}_3(t) = & D\mathbf{f}(\boldsymbol{\xi}(t), 0)\delta\mathbf{x}_3(t) \\ & + d\mathbf{f}(\boldsymbol{\xi}(t), 0)K_{\text{fl}} \left( Dg[\boldsymbol{\xi}(t)] \sum_{k=0}^{\infty} [\delta\mathbf{x}_3(t - k\tau) - \delta\mathbf{x}_3(t - (k+1)\tau)] \right) \\ & + \delta K d\mathbf{f}(\boldsymbol{\xi}(t), 0)\sigma(t) \frac{2}{1+R} z(\theta) + \mathbf{I}_3(t) z^3(\theta) \\ & - \hat{\mathbf{u}}(t) z'(\theta) - d\mathbf{f}(\boldsymbol{\xi}(t), 0)\tau K_{\text{fl}} \frac{1-R}{(1+R)^2} \sigma(t) z'(\theta) \end{aligned} \quad (18)$$

where the inhomogeneous part contributing the third power of the amplitude has been abbreviated by

$$\begin{aligned} & \mathbf{I}_3(t) \quad (19) \\ = & D^2\mathbf{f}(\boldsymbol{\xi}(t), 0) : \hat{\mathbf{u}}(t) : \mathbf{\Gamma}(t) : + Dd\mathbf{f}(\boldsymbol{\xi}(t), 0)\mathbf{\Gamma}(t)\kappa\sigma(t) \\ & + d\mathbf{f}(\boldsymbol{\xi}(t), 0)\kappa D^2g[\boldsymbol{\xi}(t)] : \hat{\mathbf{u}}(t) : \mathbf{\Gamma}(t) : + \frac{1}{6} D^3\mathbf{f}(\boldsymbol{\xi}(t), 0) : \hat{\mathbf{u}}(t) : \hat{\mathbf{u}}(t) : \hat{\mathbf{u}}(t) : \\ & + \frac{1}{2} D^2d\mathbf{f}(\boldsymbol{\xi}(t), 0) : \hat{\mathbf{u}}(t) : \hat{\mathbf{u}}(t) : \kappa\sigma(t) + \frac{1}{2} Dd^2\mathbf{f}(\boldsymbol{\xi}(t), 0)\hat{\mathbf{u}}(t)\kappa^2\sigma^2(t) \\ & + \frac{1}{6} d^3\mathbf{f}(\boldsymbol{\xi}(t), 0)\kappa^3\sigma^3(t) + \frac{1}{6} d\mathbf{f}(\boldsymbol{\xi}(t), 0)\kappa D^3g[\boldsymbol{\xi}(t)] : \hat{\mathbf{u}}(t) : \hat{\mathbf{u}}(t) : \hat{\mathbf{u}}(t) : \end{aligned}$$

We just mention that the last two terms in eq.(18) containing the derivative of the amplitude are caused by the time derivative and by the time-delayed difference evaluated in lowest order of  $\varepsilon$ . All inhomogeneous contributions to eq.(18) are antiperiodic and hence resonant. Thus a nontrivial secular condition must be imposed to ensure that  $\delta\mathbf{x}_3$  remains bounded.

To formulate such a secular condition one needs the adjoint eigenvalue equation. In view of eq.(9) the adjoint problem reads

$$\begin{aligned} & -\dot{\mathbf{v}}^\dagger(t) + i\Omega_c\mathbf{v}^\dagger(t) \\ = & \mathbf{v}^\dagger(t) \left[ D\mathbf{f}(\boldsymbol{\xi}(t), 0) + K_c \frac{1 - \exp(-i\Omega_c\tau)}{1 - R \exp(-i\Omega_c\tau)} d\mathbf{f}(\boldsymbol{\xi}(t), 0) \otimes Dg[\boldsymbol{\xi}(t)] \right] \end{aligned} \quad (20)$$

where  $\mathbf{v}^\dagger(t) = \mathbf{v}^\dagger(t + \tau)$ . For a flip instability,  $\Omega_{\text{fl}} = \pi/\tau$ , we may again reduce to real valued quantities

$$\hat{\mathbf{v}}(t) = \exp(-i\Omega_c t) \mathbf{v}^\dagger(t) \quad . \quad (21)$$

If the linear inhomogeneous equation (18) has a bounded solution, then apart from an exponentially decaying transient such a solution becomes antiperiodic,  $\delta \mathbf{x}_3(t) = -\delta \mathbf{x}_3(t + \tau)$ , because of the corresponding property of the inhomogeneous part. Thus if we multiply eq.(18) from left with  $\hat{\mathbf{v}}(t)$ , take the antiperiodicity of  $\delta \mathbf{x}_3(t)$  and the adjoint eigenvalue equation (20) into account then all the contributions containing  $\delta \mathbf{x}_3(t)$  drop when an integration over one period is performed. Only those terms coming from the inhomogeneous part survive and yield the secular condition

$$0 = \langle \hat{\mathbf{v}} | d\mathbf{f}(\boldsymbol{\xi}, 0) \sigma \rangle \frac{2}{1+R} \delta K z(\theta) + \langle \hat{\mathbf{v}} | \mathbf{I}_3 \rangle z^3(\theta) \\ - \left( \langle \hat{\mathbf{v}} | \hat{\mathbf{u}} \rangle + \langle \hat{\mathbf{v}} | d\mathbf{f}(\boldsymbol{\xi}, 0) \sigma \rangle \tau K_{\text{fl}} \frac{1-R}{(1+R)^2} \right) z'(\theta) \quad . \quad (22)$$

Here the abbreviation

$$\langle \mathbf{v} | \mathbf{u} \rangle = \frac{1}{\tau} \int_0^\tau \mathbf{v}^\dagger(t) \mathbf{u}(t) dt \quad (23)$$

denotes the usual inner product including the average over one period.

Inspecting eqs.(8) and (22) we obtain for the coefficients of the normal form the explicit expressions

$$\mu = \frac{\langle \hat{\mathbf{v}} | d\mathbf{f}(\boldsymbol{\xi}, 0) \sigma \rangle 2 / (1+R)}{\langle \hat{\mathbf{v}} | \hat{\mathbf{u}} \rangle + \langle \hat{\mathbf{v}} | d\mathbf{f}(\boldsymbol{\xi}, 0) \sigma \rangle \tau K_{\text{fl}} (1-R) / (1+R)^2} \delta K \quad (24)$$

$$r = - \frac{\langle \hat{\mathbf{v}} | \mathbf{I}_3 \rangle}{\langle \hat{\mathbf{v}} | \hat{\mathbf{u}} \rangle + \langle \hat{\mathbf{v}} | d\mathbf{f}(\boldsymbol{\xi}, 0) \sigma \rangle \tau K_{\text{fl}} (1-R) / (1+R)^2} \quad . \quad (25)$$

It is a fairly straightforward exercises to verify that the linear coefficient  $\mu$  can be expressed as  $\partial \Lambda / (\partial K)|_{K=K_{\text{fl}}} \delta K$  where the derivative denotes the derivative of the critical eigenvalue with respect to the control amplitude (cf. eq.(A.5)). In fact one already expects such a property from physical considerations without going through lengthy calculations. Thus the fraction appearing in eq.(24) has a definite sign along the flip bifurcation line. Since its numerator takes a constant value we conclude that the denominator does not change its sign along the flip bifurcation line. Therefore, since the numerator in eq.(25) is a constant, the sign of the cubic coefficient  $r$  does not change as well along the

flip bifurcation line. Thus we come to our final conclusion that no transition between sub- and supercritical behaviour appears when flip instabilities are considered (cf. the numerical results of the previous section).

The same procedure may be applied to compute the Hopf normal form and the result for the cubic coefficient looks quite similar to eq.(25). It is however the essential difference that in such a case the control parameters enter through the combination  $K_{ho}[1 - \exp(-i\Omega_{ho}\tau)]/[1 - R \exp(-i\Omega_{ho}\tau)]$  where one has to keep in mind that the critical frequency  $\Omega_{ho}$  itself is some function of the filter parameter  $R$  through the linear stability problem (cf. eq.(9)). It is mainly this dependence which makes any prediction of the sign of  $\text{Re}(r)$  a difficult task. A general expression might be of limited use in such cases. Of course numerical evaluation of such a formula is always possible but then the result certainly depends on the system under consideration.

## 4 Conclusion

The performance of time-delayed feedback control depends on whether the transitions at the control boundaries are continuous or discontinuous. Hysteresis and the associated stable and unstable coexisting solutions cause basin boundaries which may prevent stabilisation of the unstable orbit when starting from initial conditions that are not close to the target state.

By analysis of higher order codimension bifurcations we have been able to show that the associated transitions between sub- and supercritical behaviour cannot take place on control boundaries associated with flip instabilities. Thus we expect that the limitations of the control performance takes place at control boundaries where Hopf bifurcations occur, i.e. where sideband frequencies become unstable.

Since our analysis has been based on bifurcation theory it applies to quite general dynamical systems. Of course without further arguments the approach is of local nature, i.e. the analysis is a priori valid only in the vicinity of control boundaries. But the mentioned mechanism for the restriction of the basin of attraction may extend over the whole control domain. Thus our analysis has consequences for the global properties of the dynamics as well, although the implications are difficult to predict on a quantitative level.

As shown by general experience a cutoff imposed on the control force may lead to an improvement of the global control properties. According to the lines of our reasoning one may understand such a feature on an analytical level, i.e. subcritical transitions and the associated constraints on basins of attraction are suppressed. Of course more detailed investigations are required. But with

the presented tools one may tackle such a problem.

In order to improve the control performance discontinuous transitions at the control boundaries have to be avoided. A closer look at the analytical expressions of the normal form may result in recipes how such a goal can be reached, i.e. by certain modifications for the feedback of the control signal  $s(t) - s(t - \tau)$ . A deeper analysis in such a direction is desirable.

Last but not least further numerical and in particular experimental investigations are required to demonstrate the universality and relevance of the proposed mechanism. Fortunately that is quite simple on the phenomenological level since discontinuous transitions and hysteresis can be easily studied directly by observing the control signal. The occurrence of such a feature should be related to a decrease in control performance. For instance small basins of attraction may be reflected by an increased sensitivity of the control system with respect to noise. In fact, these features have been found in preliminary electronic circuit experiments. Details will be published elsewhere.

## Acknowledgement

Support by the German Research Foundation through grants no. JU 261/3-1 and BE 864/4-1 is gratefully acknowledged.

## A Derivative of eigenvalues

Consider the eigenvalue problem for time-delayed feedback control and the adjoint equation (cf. eqs.(9) and (20)) for general parameter values

$$\begin{aligned} & \Lambda \mathbf{u}(t) + \dot{\mathbf{u}}(t) \\ &= D\mathbf{f}(\boldsymbol{\xi}(t), 0)\mathbf{u}(t) + d\mathbf{f}(\boldsymbol{\xi}(t), 0)K \frac{1 - \exp(-\Lambda\tau)}{1 - R \exp(-\Lambda\tau)} Dg[\boldsymbol{\xi}(t)]\mathbf{u}(t) \quad (\text{A.1}) \end{aligned}$$

$$\begin{aligned} & \Lambda \mathbf{v}^\dagger(t) - \dot{\mathbf{v}}^\dagger(t) \\ &= \mathbf{v}^\dagger(t) D\mathbf{f}(\boldsymbol{\xi}(t), 0) + \mathbf{v}^\dagger(t) d\mathbf{f}(\boldsymbol{\xi}(t), 0)K \frac{1 - \exp(-\Lambda\tau)}{1 - R \exp(-\Lambda\tau)} Dg[\boldsymbol{\xi}(t)] \quad (\text{A.2}) \end{aligned}$$

Taking the derivative of eq.(A.1) with respect to  $K$  (for  $R$  fixed) we obtain

$$\frac{\partial \Lambda}{\partial K} \mathbf{u}(t) + \Lambda \frac{\partial \mathbf{u}}{\partial K} + \frac{d}{dt} \left( \frac{\partial \mathbf{u}}{\partial K} \right)$$

$$\begin{aligned}
&= D\mathbf{f}(\boldsymbol{\xi}(t), 0) \frac{\partial \mathbf{u}}{\partial K} + d\mathbf{f}(\boldsymbol{\xi}(t), 0) K \frac{1 - \exp(-\Lambda\tau)}{1 - R \exp(-\Lambda\tau)} Dg[\boldsymbol{\xi}(t)] \frac{\partial \mathbf{u}}{\partial K} \\
&\quad + d\mathbf{f}(\boldsymbol{\xi}(t), 0) \frac{\partial}{\partial K} \left( K \frac{1 - \exp(-\Lambda\tau)}{1 - R \exp(-\Lambda\tau)} \right) Dg[\boldsymbol{\xi}(t)] \mathbf{u}(t) \quad . \quad (\text{A.3})
\end{aligned}$$

Multiplication with  $\mathbf{v}^\dagger(t)$  yields taking the adjoint equation (A.2) into account

$$\begin{aligned}
&\frac{\partial \Lambda}{\partial K} \mathbf{v}^\dagger(t) \mathbf{u}(t) + \frac{d}{dt} \left( \mathbf{v}^\dagger(t) \frac{\partial \mathbf{u}}{\partial K} \right) \\
&= \mathbf{v}^\dagger(t) d\mathbf{f}(\boldsymbol{\xi}(t), 0) \frac{\partial}{\partial K} \left( K \frac{1 - \exp(-\Lambda\tau)}{1 - R \exp(-\Lambda\tau)} \right) Dg[\boldsymbol{\xi}(t)] \mathbf{u}(t) \quad . \quad (\text{A.4})
\end{aligned}$$

If we finally integrate over one period we end up with

$$\begin{aligned}
&\frac{\partial \Lambda}{\partial K} \left( \langle \mathbf{v} | \mathbf{u} \rangle - \langle \mathbf{v} | d\mathbf{f}(\boldsymbol{\xi}, 0) (Dg[\boldsymbol{\xi}] \mathbf{u}) \rangle \frac{\tau(1 - R) \exp(-\Lambda\tau)}{[1 - R \exp(-\Lambda\tau)]^2} \right) \\
&= \frac{1 - \exp(-\Lambda\tau)}{1 - R \exp(-\Lambda\tau)} \langle \mathbf{v} | d\mathbf{f}(\boldsymbol{\xi}, 0) (Dg[\boldsymbol{\xi}] \mathbf{u}) \rangle \quad . \quad (\text{A.5})
\end{aligned}$$

## References

- [1] E. Ott, C. Grebogi, and Y. A. Yorke, *Controlling Chaos*, Phys. Rev. Lett. **64**, 1196 (1990).
- [2] R. Bellmann, *Dynamic programming and modern control theory* (Acad. Press, New York, 1965).
- [3] H. Nijmeijer and A. Schaft, *Nonlinear Dynamical Control Systems* (Springer, New York, 1996).
- [4] K. Ogata, *Modern Control Engineering* (Prentice–Hall, New York, 1997).
- [5] T. Shinbrot, *Progress in the control of chaos*, Adv. Phys. **44**, 73 (1995).
- [6] K. Pyragas, *Continuous control of chaos by self–controlling feedback*, Phys. Lett. A **170**, 421 (1992).
- [7] O. Lüthje, S. Wolff, and G. Pfister, *Control of Chaotic Taylor–Couette Flow with Time–Delayed Feedback*, Phys. Rev. Lett. **86**, 1745 (2001).
- [8] S. Bielawski, D. Derozier, and P. Glorieux, *Experimental characterization of unstable periodic orbits by controlling chaos*, Phys. Rev. A **47**, R2492 (1993).
- [9] H. Benner and W. Just, *Control of chaos by time delayed feedback in high power ferromagnetic resonance experiments*, J. Kor. Phys. Soc. **40**, 1046 (2002).

- [10] P. Parmananda, R. Madrigal, M. Rivera, L. Nyikos, I. Z. Kiss, and V. Gáspár, *Stabilization of unstable steady states and periodic orbits in an electrochemical system using delayed-feedback control*, Phys. Rev. E **59**, 5266 (1999).
- [11] J. K. Hale and S. M. Verduyn Lunel, *Introduction to Functional Differential Equations* (Springer, New York, 1993).
- [12] M. E. Bleich and J. E. S. Socolar, *Controlling spatiotemporal dynamics with time-delayed feedback*, Phys. Rev. E **54**, R17 (1996).
- [13] H. Nakajima, *On analytical properties of delayed feedback control of chaos*, Phys. Lett. A **232**, 207 (1997).
- [14] W. Just, T. Bernard, M. Ostheimer, E. Reibold, and H. Benner, *Mechanism of time-delayed feedback control*, Phys. Rev. Lett. **78**, 203 (1997).
- [15] *Handbook of Chaos Control*, edited by H. G. Schuster (Wiley-VCH, Berlin, 1999).
- [16] Y.-C. Lai, C. Grebogi, J. A. Yorke, and S. C. Venkataramani, *Riddling Bifurcation in Chaotic Dynamical Systems*, Phys. Rev. Lett. **77**, 55 (1996).
- [17] B. Krauskopf and K. Green, *Computing unstable manifolds of periodic orbits in delay differential equations*, J. Comp. Phys. **186**, 230 (2003).
- [18] W. Just, E. Reibold, H. Benner, K. Kacperski, F. Fronczak, and J. Hołyst, *Limits of time-delayed feedback control*, Phys. Lett. A **254**, 158 (1999).
- [19] W. Just, H. Benner, and E. Reibold, *Theoretical and experimental aspects of chaos control by time-delayed feedback*, Chaos **13**, 259 (2003).
- [20] J. E. S. Socolar, D. W. Sukow, and D. J. Gauthier, *Stabilizing unstable periodic orbits in fast dynamical systems*, Phys. Rev. E **50**, 3245 (1994).
- [21] O. Beck, A. Amann, E. Schöll, J. E. S. Socolar, and W. Just, *Comparison of time-delayed feedback schemes for spatio-temporal control of chaos in a reaction-diffusion system with global coupling*, Phys. Rev. E **66**, 016213 (2002).
- [22] F. Giannakopoulos and A. Zapp, *Bifurcations in a planar system of differential delay equations modeling neural activity*, Physica D **159**, 215 (2001).
- [23] B. F. Redmond, V. G. LeBlanc, and A. Longtin, *Bifurcation analysis of a class of first-order nonlinear delay-differential equations with reflectional symmetry*, Physica D **166**, 131 (2002).
- [24] M. Schanz and A. Pelster, *Analytical and numerical investigations of the phase-locked loop with time delay*, Phys. Rev. E **67**, 056205 (2003).